Compton Scattering with a ^{137}Cs source

Lei Katherine, Fortin Clément, Amar Selim

McGill University Department of Physics

Supervisor: Professor Dominic Ryan, Professor Peter Grütter

January 21, 2022

Abstract

A Compton scattering experiment is presented. A NaI(TI) scintillating crystal paired with a photomultiplier tube is used as the photon detector and a multichannel analyzer is used to register the counts. Sources of known energy (^{133}Ba, ^{57}Co, ^{22}Na and ^{137}Cs) are used for calibration. A preliminary calibration is obtained, suggesting a linear relationship of $E = m \cdot channel + b$ with $m = 0.37(2)$ KeV/channel, $b = -6(^{+3}_{-20})$ KeV. Scattering data on an aluminium road is then taken for 6 scattering angles paired with background data. Using this, a first estimate for the rest mass energy of the electron is obtained: $m_e c^2 = 513(2)$ KeV. Finally, future plans are given, which include estimating systematic uncertainties, getting a definitive value for the rest mass energy of the electron and comparing the Thomson and Klein-Nishina predictions for the cross section.

Contents

1 Apparatus and Calibration

1.1 Equipment and Setup

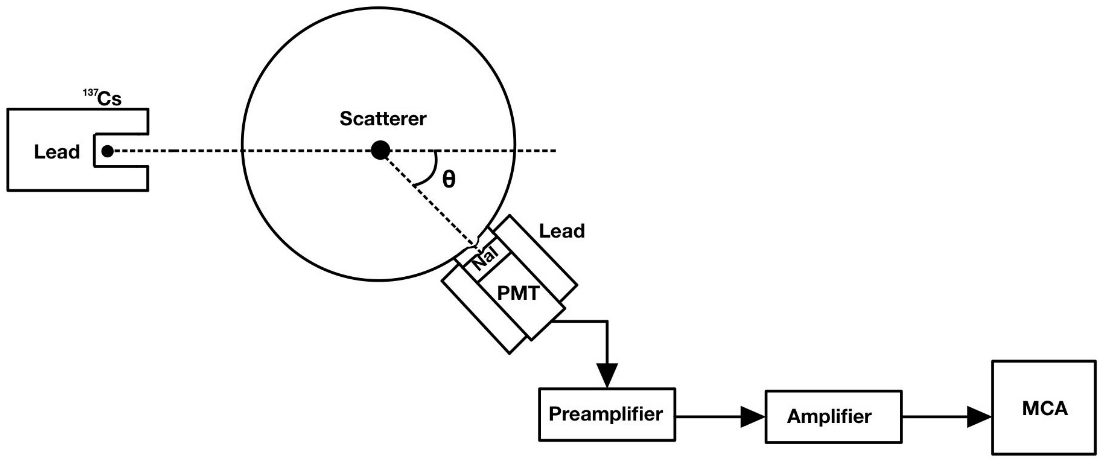

Figure 1: A schematic diagram of the experimental arrangement for measuring the Compton scattering of ^{137}Cs gamma rays from different scattering targets, comprising a ^{137}Cs source of 661.6 KeV gamma ray, lead shields, interchangeable scattering rod, a detection circuit comprising a a NaI(Tl) scintillating crystal (Bicron [1]) on a rotating arm coupled to a photomultiplier tube (PMT) biased at V_bias (Ortec 459 [2]), a preamplifier (Ortec 113 [3]), a pulseshaping amplifier (Canberra 816 [4]), and a multichannel analyzer (MCA, Ortec Easy-MCA-2k [5]).

To measure the energy of the scattered photons, we use a multichannel analyzer (MCA, Ortec Easy-MCA-2k) that maps voltage to a channel number linearly related to the energy of the detected photons. Figure 1 shows a schematic diagram of our apparatus.

A NaI(Tl) scintillating crystal is positioned at an angle θ away from the line connecting the Cs-137 source and the scattering rod. When the gamma ray hits the crystal, it produces scintillated photons. Some of them then come in contact with the active surface of the PMT and produce electrons through the photoelectric effect. The PMT amplifies these electrons into a discernible current pulse which is then converted to a voltage pulse by the preamplifier, and then further amplified and shaped by the amplifier. Finally, the MCA maps the peak voltage onto one of the 2048 channels available. The right panel of fig. 2 shows the number of times each channel has been mapped to over a 30 seconds interval for a ^{57}Co source.

1.2 Calibration

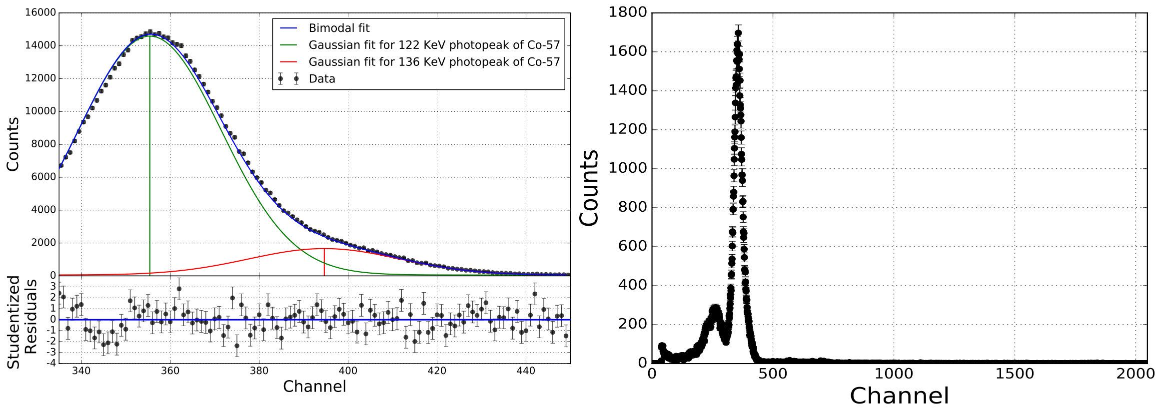

Figure 2: Left: A bimodal distribution (blue) with each mode (green and red) fitted over the channel range [335,450] of 5 minutes of ^{57}Co data with Poisson uncertainty. The green mode peaking at 355.4(2) corresponds to the 122 KeV photopeak while the red mode peaking at 395(5) corresponds to 136 KeV. The reduced chi-squared is 1.2(1). Right: Data for a 30 seconds time interval for ^{57}Co. The highest peak includes the two photopeaks while the smaller one on its left is of unknown origin and thus was not used in the calibration.

To measure the scattered photons' energy, the relationship between energy and channel number need first be determined. This is done by collecting photon counts for four different sources with known gamma photopeaks [6–9]: ^{137}Cs, ^{133}Ba, ^{57}Co and ^{22}Na. To identify peaks in channel number, Gaussian functions are fitted using least-square methods together with a background function trying to take into account any potential noise or influence from other nearby peaks. While for some a constant background function was enough to get rid of any structure in the residuals, the 31 KeV peak of ^{133}Ba in the channel region [50,130] required a linear background function and Cobalt 57 required instead a Bimodal fit (i.e., two Gaussians), as shown on the left panel of fig. 2. In the latter case, it allowed us to identify the smaller-intensity peak at 136 KeV. The bimodal fit yields a reduced chi-squared of 1.2(1), indicating good agreement with the data and justifying the inclusion of the 136 KeV peak. Though other background functions have been tested, such as polynomials, they were seen to poorly fit the data under consideration. As for the statistical uncertainties, they are set from the assumptions that the underlying distribution is Poisson, i.e. an uncertainty of $\sqrt{N}$ on N counts.

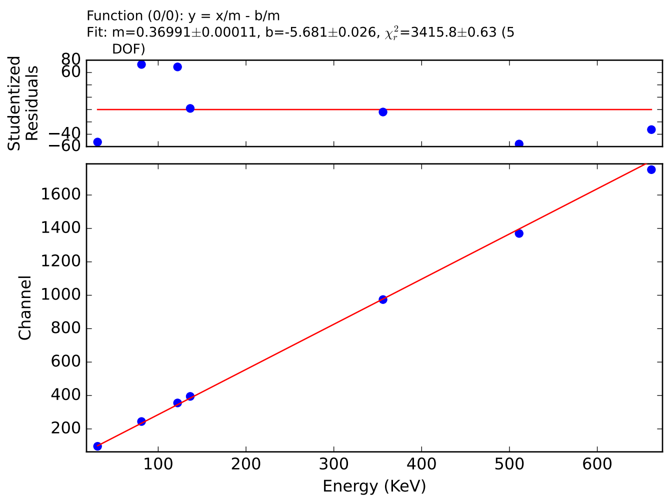

Figure 3: Locations of the 7 channel peaks against their known energy. The fit parameters $m = 0.37(2)$ KeV/channel and $b = -6(^{+3}_{-20})$ KeV give the linear relationship $E = m \cdot ch + b$ with a reduced chi-squared of 3415.8(6). The systematic uncertainties on the channels are believed to be underestimated leading to high reduced chi-squared and studentized residuals.

For each calibrating source, we plotted the peak channel number determined from the Gaussian fits against their corresponding energy values obtained from [6–9]. The statistical uncertainties in the peaks' locations were obtained from the Gaussian fits while the systematic uncertainties were estimated as the standard deviation of the distribution of peak locations we obtained when varying the channel region in which we were fitting. By fitting a linear function of the form of $y = x/m - b/m$ for channel against energy, we obtained the relationship $energy = m \times channel + b$ where $m = 0.37(2)$ KeV/channel and $b = -6(^{+3}_{-20})$ KeV, as shown in 3. The systematic uncertainty was estimated by removing some data points and computing how m and b vary. Although the linear function captures the behaviour of our data, the reduced chi-squared yields 3415.8(6) and the studentized residuals are mostly on the order of 50 which might be due to underestimation of the systematic uncertainties of our peak channels, since the data points exhibit a clear linear relationship. Sources of systematic uncertainty are not yet fully identified, but candidates are our choice of background functions and the effects of small-intensity photopeaks on the ones we considered. These could come from unknown origins, such as the fictitious peak in the channel region [250,330] of ^{57}Co, or directly from the source. Since we know the spectrum of our sources, we can locate the smaller peaks coming from them and determine whether they affect our results. Lastly, the relationship might not entirely be linear and small corrections such as a quadratic term could improve the fit. These possibilities will be explored in the future, see section 2.

2 Progress summary and future plans

2.1 Progress up to January 20^{th}

1. We fitted Gaussian functions to 7 photopeaks of our calibrating sources while identifying the appropriate background functions to use for each of them. We also got a first estimate of the systematic uncertainty in their channel location by varying the regions in which we're fitting.

2. We used these 7 peaks to find the relationship between energy and channel (calibration).

3. We collected scattering data on an aluminium rod and background data for 6 angles (from 40° to 100°) and used it with our calibration to make a first plot of the energy of the scattered photon as a function of the scattering angle 4. It gave a first estimate of 513(2) KeV for the rest mass energy of the electron, in agreement with the known value. This should not be taken as a result but only as a demonstration of our progress.

Plots and fits were done using the spinmob and mcphysics Python packages and the code was organized in a GitHub repository for future uses.

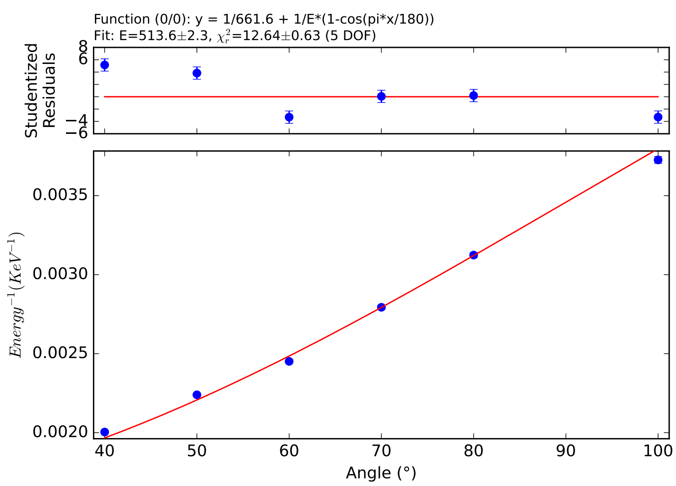

Figure 4: Inverse of the energy of the scattered photon against the scattered angle[a]. It gives an estimate for the rest mass energy of the electron of $m_e c^2 = 513(2) KeV$. The reduced chi-squared is 12.6(6) and some of the studentized residuals are of order ≈ 5 which suggests a poor fit.

[a] This plot doesn't include the systematic uncertainty in the calibration parameters m and b as we want a better estimate of these uncertainties before using them here.

2.2 Future plans

1. Get more accurate estimates of the locations of the peaks and their systematic uncertainties by determining if small-intensity photopeaks are interfering with our fits and estimating their effects using multimodal fits. To better determine our systematic uncertainties, we are also thinking of varying our choice of background functions as a means to quantify the systematic uncertainty it causes in the photopeaks' locations.

2. Redo the calibration with those new fit parameters and uncertainties; if the linear fit has not improved, we shall evaluate the possibility of a quadratic term. Furthermore, we want to improve our estimate of the systematic uncertainty on the parameters m and b as it seems overestimated right now (particularly for b).

3. Get a better fit of energy versus angle by treating the Gaussian fits for Aluminum more carefully—we've remarked that a lot of them were quite poor. To improve our estimate for the electron rest mass energy, we shall collect more scattering data, try different background functions and change the initial guesses for the fitting parameters. We will also include the systematic uncertainties of m and b in the fit.

4. Start thinking about how we will obtain the total detection rate of photons from our data. In particular, how to account for the detector's efficiency. Using this data, we wish to compare Thomson and Klein-Nishina predictions for the cross section and see which agrees more with the data.

5. Use our detection rate data and estimates of other necessary variables (incident beam intensity, solid angle of our detectors, physical constants) to measure the electron density of one or more scattering elements. We could do this by using one element to estimate the necessary variables and then measure the electron density of another.

Even if the calibration doesn't improve dramatically, we are still planning to carry on with the 3rd point since we do not believe that the accuracy in our calibration is the main source of problems in our fit of energy versus angle. Rather, the poor Gaussian fits are certainly the culprits. We will of course keep track of our progress in our logbook.

References

[1] S.-G. Crystals. (2005) NaI(TI) and Polyscin® NaI(TI) Sodium Iodide Scintillation Material. [Online]. Available: https://www.crystals.saint-gobain.com/sites/hps-mac3-cma-crystals/files/2021-08/Sodium-Iodide-Material-Data-Sheet.pdf 1

[2] Ortec. (2002) 266 Photomultiplier Base. [Online]. Available: https://www.ortec-online.com/products/electronics/photomultiplier-tube-bases/266 1

[3] Ortec. (2002) 113 Scintillation Preamplifier. [Online]. Available: https://www.ortec-online.com/products/electronics/preamplifiers/113 1

[4] Canberra. Spectroscopy Amplifier Model 816. [Online]. Available: http://www.nuclearphysicslab.com/npl/wp-content/uploads/Canberra_816_Spectroscopy_Amplifier.pdf 1

[5] Ortec. (2014) Easy-MCA 2k or 8k Channel Multichannel Analyzer. [Online]. Available: https://www.ortec-online.com/products/electronics/multichannel-analyzers-mca/basic-analog/easy-mca-2k-or-8k 1

[6] Y. Khazov, A. Rodionov, and F. Kondev, "Nuclear Data Sheets for A = 133," *Nuclear Data Sheets*, vol. 112, no. 4, pp. 855–1113, 2011. [Online]. Available: https://www.sciencedirect.com/science/article/pii/S0090375211000202 2, 3

[7] M. R. Bhat, "Nuclear Data Sheets for A = 57," *Nucl. Data Sheets*, vol. 85, pp. 415–536, 1998. [Online]. Available: https://www.sciencedirect.com/science/article/abs/pii/S0090375298900217?via%3Dihub 2, 3

[8] E. Browne and J. Tuli, "Nuclear Data Sheets for A = 137," *Nuclear Data Sheets*, vol. 108, no. 10, pp. 2173–2318, 2007. [Online]. Available: https://www.sciencedirect.com/science/article/pii/S0090375207000804 2, 3

[9] M. S. Basunia, "Nuclear Data Sheets for A = 22," *Nuclear Data Sheets*, vol. 127, pp. 69–190, 2015. [Online]. Available: https://www.sciencedirect.com/science/article/pii/S0090375215000253 2, 3